The Formation and Evolution of Africa

A Synopsis of 3.8 Ga of Earth History

Edited by
D. J. J. van Hinsbergen, S. J. H. Buiter, T. H. Torsvik, C. Gaina and S. J. Webb

Geological Society
Special Publication 357

Geological Society books refereeing procedures

The Society makes every effort to ensure that the scientific and production quality of its books matches that of its journals. Since 1997, all book proposals have been refereed by specialist reviewers as well as by the Society's Books Editorial Committee. If the referees identify weaknesses in the proposal, these must be addressed before the proposal is accepted.

Once the book is accepted, the Society Book Editors ensure that the volume editors follow strict guidelines on refereeing and quality control. We insist that individual papers can only be accepted after satisfactory review by two independent referees. The questions on the review forms are similar to those for *Journal of the Geological Society*. The referees' forms and comments must be available to the Society's Book Editors on request.

Although many of the books result from meetings, the editors are expected to commission papers that were not presented at the meeting to ensure that the book provides a balanced coverage of the subject. Being accepted for presentation at the meeting does not guarantee inclusion in the book.

More information about submitting a proposal and producing a book for the Society can be found on its web site: www.geolsoc.org.uk.

It is recommended that reference to all or part of this book should be made in one of the following ways:

Van Hinsbergen, D. J. J., Buiter, S. J. H., Torsvik, T. H., Gaina, C. & Webb, S. J. (eds) 2011. *The Formation and Evolution of Africa: A Synopsis of 3.8 Ga of Earth History.* Geological Society, London, Special Publications, **357**.

Letts, S., Torsvik, T. H., Webb, S. J. & Ashwal, L. D. 2011. New Paleoproterozoic palaeomagnetic data from the Kaapvaal Craton, South Africa. *In*: Van Hinsbergen, D. J. J., Buiter, S. J. H., Torsvik, T. H., Gaina, C. & Webb, S. J. (eds) *The Formation and Evolution of Africa: A Synopsis of 3.8 Ga of Earth History.* Geological Society, London, Special Publications, **357**, 9–26.

GEOLOGICAL SOCIETY SPECIAL PUBLICATION NO. 357

The Formation and Evolution of Africa: A Synopsis of 3.8 Ga of Earth History

EDITED BY

D. J. J. VAN HINSBERGEN
University of Oslo, Norway

S. J. H. BUITER
Geological Survey of Norway

T. H. TORSVIK
University of Oslo

C. GAINA
Geological Survey of Norway

and

S. J. WEBB
University of the Witwatersrand, South Africa

2011
Published by
The Geological Society
London

THE GEOLOGICAL SOCIETY

The Geological Society of London (GSL) was founded in 1807. It is the oldest national geological society in the world and the largest in Europe. It was incorporated under Royal Charter in 1825 and is Registered Charity 210161.

The Society is the UK national learned and professional society for geology with a worldwide Fellowship (FGS) of over 10 000. The Society has the power to confer Chartered status on suitably qualified Fellows, and about 2000 of the Fellowship carry the title (CGeol). Chartered Geologists may also obtain the equivalent European title, European Geologist (EurGeol). One fifth of the Society's fellowship resides outside the UK. To find out more about the Society, log on to www.geolsoc.org.uk.

The Geological Society Publishing House (Bath, UK) produces the Society's international journals and books, and acts as European distributor for selected publications of the American Association of Petroleum Geologists (AAPG), the Indonesian Petroleum Association (IPA), the Geological Society of America (GSA), the Society for Sedimentary Geology (SEPM) and the Geologists' Association (GA). Joint marketing agreements ensure that GSL Fellows may purchase these societies' publications at a discount. The Society's online bookshop (accessible from www.geolsoc.org.uk) offers secure book purchasing with your credit or debit card.

To find out about joining the Society and benefiting from substantial discounts on publications of GSL and other societies worldwide, consult www.geolsoc.org.uk, or contact the Fellowship Department at: The Geological Society, Burlington House, Piccadilly, London W1J 0BG: Tel. +44 (0)20 7434 9944; Fax +44 (0)20 7439 8975; E-mail: enquiries@geolsoc.org.uk.

For information about the Society's meetings, consult *Events* on www.geolsoc.org.uk. To find out more about the Society's Corporate Affiliates Scheme, write to enquiries@geolsoc.org.uk.

Published by The Geological Society from:
The Geological Society Publishing House, Unit 7, Brassmill Enterprise Centre, Brassmill Lane, Bath BA1 3JN, UK

(*Orders*: Tel. +44 (0)1225 445046, Fax +44 (0)1225 442836)
Online bookshop: www.geolsoc.org.uk/bookshop

British Library Cataloguing in Publication Data

A catalogue record for this book is available from the British Library.
ISBN 978-1-86239-335-6

Distributors
For details of international agents and distributors see:
www.geolsoc.org.uk/agentsdistributors

Typeset by Techset Composition Ltd, Salisbury, UK
Printed by MPG Books Ltd, Bodmin, UK

Contents

The enigmatic Chad lineament revisited with global gravity and gravity-gradient fields

CARLA BRAITENBERG[1]*, PATRIZIA MARIANI[1], JÖRG EBBING[2,3] & MICHAL SPRLAK[1,4]

[1]*Dipartimento di Geoscienze, Università di Trieste, via Weiss 1, 34100 Trieste, Italy*

[2]*Geological Survey of Norway (NGU), Leiv Eirikssons vei 39, 7491 Trondheim*

[3]*Department of Petroleum Engineering and Applied Geophysics, NTNU, 7491 Trondheim, Norway*

[4]*Research Institute of Geodesy and Cartography, Chlumeckého 4, 826 62 Bratislava, Slovakia*

**Corresponding author (e-mail: berg@units.it)*

Abstract: The crustal structure of northern Africa is puzzling, large areas being of difficult access and concealed by the Sahara. The new global gravity models are of unprecedented precision and spatial resolution and offer a new possibility to reveal the structure of the lithosphere beneath the Sahara. The gravity gradients correlate better than gravity with geological features such as rifts, fold belts and magmatic deposits and intrusions. They are an ideal tool to follow geological units (e.g. basement units) below a stratigraphic layer of varying density (e.g. sediments). We focus on the Chad lineament, a 1300 km arcuate feature located between the west and central African rift system. The gravity fields show differences between the lineament and the west and central African rift system. Along the centre of the lineament high-density rocks must be present, which relate to either magmatic or metamorphic rocks. This is very different to the lineaments of the western and central-west African rift system which are filled with sediments. Considering present models of rifting and the absence of topography, the lineament cannot be coeval to the west and central African rift system and is most likely older. We suggest that the lineament is a structural element of the Saharan Metacraton.

Geodetic satellite missions, for example CHAMP (CHAllenging Mini-Satellite Payload), GRACE (Gravity Recovery And Climate Experiment) and GOCE (Gravity field and steady-state Ocean Circulation Explorer), have been flown in recent years to map the Earth's gravity field to an unprecedented precision and spatial resolution. Preliminary data of the GOCE mission are now available, but with lower spatial resolution than global models based on the observations of satellite data combined with terrestrial data (e.g. Rummel *et al.* 2002; Förste *et al.* 2008). Terrestrial data include observations acquired by a gravimeter on land, ship and airplane; altimeter satellite observations of the sea surface also contribute to terrestrial observations, because the sea surface follows the geoid. The global satellite-terrestrial gravity field models are available in spherical harmonic expansion with maximum degree and order of $N = 360$ (EIGEN05C – European Improved Gravity model of the Earth by New techniques; Förste *et al.* 2008) or $N = 2159$ (EGM2008 – Earth Gravitational Model 2008; Pavlis *et al.* 2008). The preliminary model derived with GOCE observations is only available with $N = 210$, 224 or 250, according to different calculation methods (Bruinsma *et al.* 2010; Migliaccio *et al.* 2010; Pail *et al.* 2010). The maximum degree and order of the expansion is an important parameter, because a higher degree will show smaller-scale structures. By subtracting the potential field of the reference ellipsoid from the Earth's gravity potential, the disturbing potential is obtained. The disturbing potential represents the gravity effect of the density variations inside the Earth with respect to a homogeneous ellipsoid. The gravity anomaly is equal to the first spatial derivative, and the gravity-gradient tensor (Marussi tensor) is equal to the second derivatives of the disturbing potential (e.g. Hofmann-Wellenhof & Moritz 2005).

In the present study we calculate the gravity anomaly and the gravity gradients for north-central Africa, using the global model EGM2008 which has the highest spatial resolution. We show that the fields have sufficient spatial resolution and accuracy to detect geological boundaries. We compare the gravity signals to a schematic geological map of north-central Africa that includes those features which are presumably accompanied by density variations. The wavelengths of the geological units must

From: VAN HINSBERGEN, D. J. J., BUITER, S. J. H., TORSVIK, T. H., GAINA, C. & WEBB, S. J. (eds) *The Formation and Evolution of Africa: A Synopsis of 3.8 Ga of Earth History*. Geological Society, London, Special Publications, **357**, 329–341. DOI: 10.1144/SP357.18 0305-8719/11/$15.00

be larger than the spatial resolution of the gradient fields, in order to be detected. We seek the relationship between the gravity signals and the different geological structures, in order to demonstrate that the fields can be used to identify geological units. This knowledge can be transferred to areas in which the geology is not well known (e.g. Braitenberg & Ebbing 2009), in order to guide future geological campaigns and determine geological boundaries.

Another application is to investigate outcropping structures by tracing the gravity signal. A good example is the arched gravity anomaly in eastern Chad, which had been noticed in the early 1970s (e.g. Louis 1970). In our work we compare the characteristics of the linear anomaly, which we call the Chad lineament, with the gravity signal of the central African rift and the Pan-African suture. The present data are more complete with respect to the studies of the 1960s and 1970s, because the terrestrial data have been merged with satellite observations allowing the anomaly to be viewed in a regional context. Previous interpretations associated the anomaly either with a rift or a suture; we show that the lineament differs in several aspects from the nearby rifts and thus is not a coeval rift. We discuss the other possible interpretations.

Satellite and terrestrial gravity field

Nominally the smallest wavelength resolvable with the EGM2008 potential field model is equal to $\lambda_{min} = 2\pi R/N_{max} = 19$ km (Hofmann-Wellenhof & Moritz 2005), where R is Earth's radius and N_{max} is the maximum degree and order of the expansion. The spatial wavelengths of EGM08 longer than 572 km (maximal degree and order of spherical harmonic expansion $N = 70$), which correspond to features greater than 286 km (half wavelength), are based entirely on satellite observations and are therefore truly global (Förste *et al.* 2008). Wavelengths between 572 ($N = 70$) and 334 km ($N = 120$) depend increasingly on terrestrial data, whereas wavelengths smaller than 334 km ($N = 120$) depend entirely on terrestrial data. For the GOCE-derived model, wavelengths down to *c.* 191 km ($N = 210$) are resolved and are ideal for testing the validity of the EGM08 model. In terms of degree of the spherical harmonic expansion, EGM08 relies entirely on terrestrial data for degrees between $N = 120$ and $N = 2159$. The GOCE model allows us to control the EGM08 field up to degree $N = 210$, that is, we are testing the contribution of terrestrial data between $N = 120$ and $N = 210$. A good correspondence between the two fields allows us to be confident that up to degree 210 terrestrial data correctly represent the field, and gives us confidence in the correctness of the higher orders.

In Figure 1 the gravity anomaly derived from the GOCE satellite (Migliaccio *et al.* 2010) is compared to the gravity anomaly derived from the EGM08 model (Pavlis *et al.* 2008). Among the three available GOCE models we choose the space-wise solution (Migliaccio *et al.* 2010), which takes advantage of the spatial correlation of the gravity field by applying a local numerical solution method to produce intermediate grid data; for this reason, it is expected that it can better describe local or regional behaviour of the field. The fields are in good agreement and only differ slightly in a few places, which is due to the varying density of terrestrial data. The statistical parameters for the difference between the two fields are: average difference = 0.02 mGal, standard deviation = 6 mGal, maximal value of difference = 36 mGal. The only evident mismatch is found in Nigeria (longitude 7°, latitude 10°): a high-gravity value is found in EGM08 (bright red spot) which is missing in the GOCE field, and is therefore probably due to a confined problem in the terrestrial data used in EGM08.

The use of satellite data in north Africa is particularly useful, because the combination of different terrestrial gravity campaigns is hampered since a unified height system is not available everywhere; the combined fields therefore may have errors in the wavelength range equal to multiples of the individual length scale of the campaign.

Ideally, all data are linked to the reference system ISGN71 (International Gravity Standardization Net 1971) which provides absolute reference stations. ISGN71 has a bias to western countries however, where the number of available absolute gravity stations is of greater density. The gravimeter being a relative instrument, measurements must always start at an absolute gravity station in order to reduce the gravity differences to gravity values. Some datasets are therefore linked to a reference station which is far away and are only linked internally. In such cases, a long-wavelength shift might occur. This problem is relieved with the global gravity fields that merge the terrestrial data using the control on the longer wavelengths through the satellite data. A further advantage of the global availability of the potential field is to be able to calculate the gradient tensor, a quantity well-suited for highlighting upper crustal density. The terrestrial data nonetheless are important in defining wavelengths shorter than 334 km of the EGM08 field.

The gradient field or Marussi tensor

The gravity-potential field EGM2008 (Pavlis *et al.* 2008) is published in terms of the spherical harmonic expansion, for which spherical coordinates are

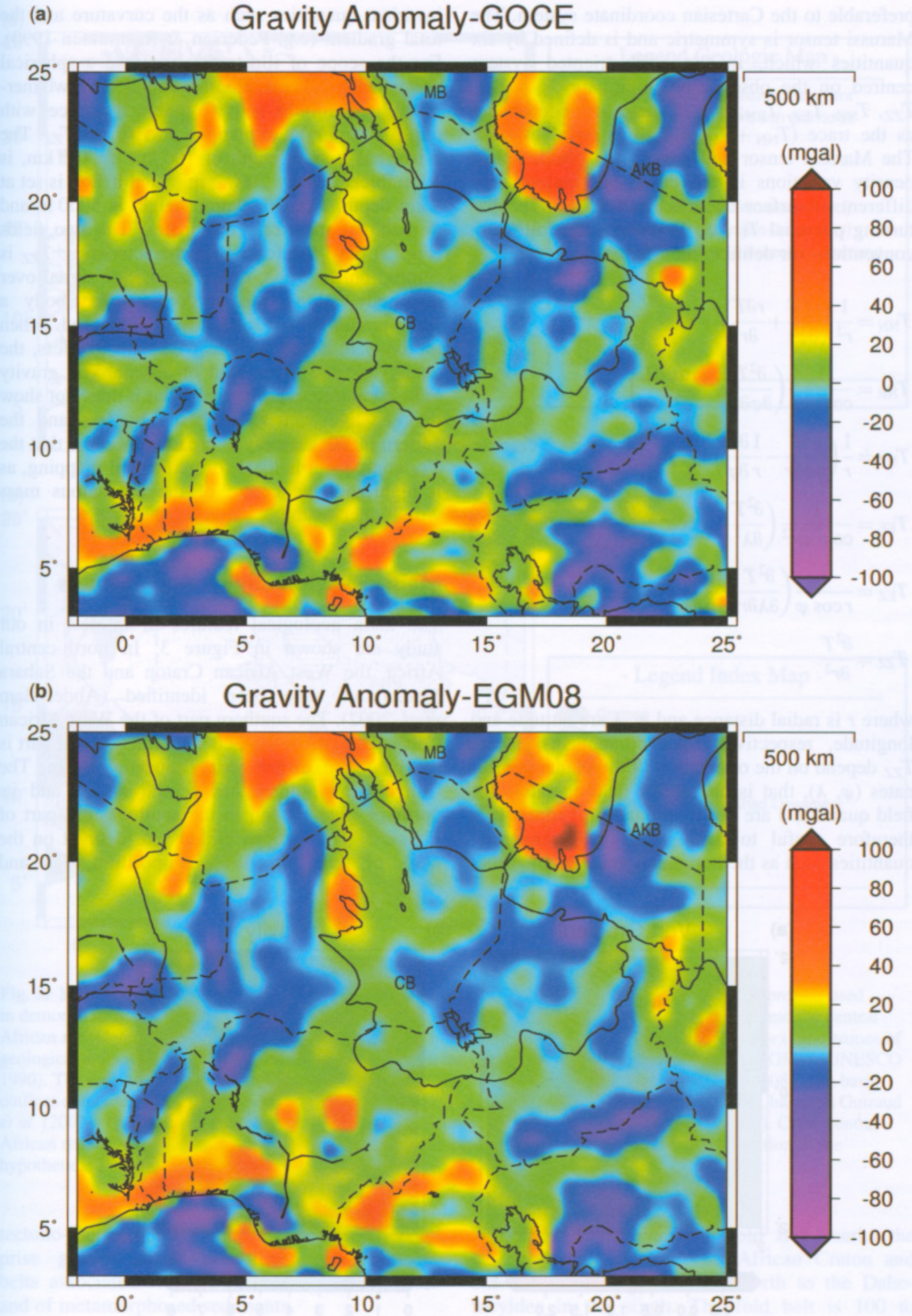

Fig. 1. Control of the combined terrestrial-satellite gravity model with a truly global satellite-derived gravity model. Maximum degree and order $N = 210$. (**a**) Gravity anomaly observed from satellite GOCE (Migliaccio *et al.* 2010) and (**b**) combined satellite-terrestrial gravity model EGM08 (Pavlis *et al.* 2008). CB, Chad basin; MB, Murzuk basin; AKB, Al Kufra basin. Outlines of major sedimentary basins depicted as continuous line; national borders depicted as dashed line.

preferable to the Cartesian coordinate system. The Marussi tensor is symmetric and is defined by six quantities which, in the north-oriented system centred on the observation point, are T_{NN}, T_{EE}, T_{ZZ}, T_{NZ}, T_{EZ}, T_{EN}; five of these are independent as the trace $(T_{NN}+T_{EE}+T_{ZZ})$ is equal to zero. The Marussi tensor and gravity field both reflect density variations in the crust, but outline very different subsurface features. Starting from the disturbing potential $T(r, \varphi, \lambda)$ we use the following conventions for defining the Marussi tensor:

$$T_{NN}=\frac{1}{r^2}\left(\frac{\partial^2 T}{\partial\varphi^2}+\frac{r\partial T}{\partial r}\right)$$

$$T_{NE}=\frac{1}{\cos\varphi r^2}\left(\frac{\partial^2 T}{\partial\varphi\partial\lambda}+\frac{\tan\varphi\partial T}{\partial\lambda}\right)=T_{EN}$$

$$T_{NZ}=\frac{1}{r}\left(\frac{\partial^2 T}{\partial\varphi\partial r}-\frac{1}{r}\frac{\partial T}{\partial\varphi}\right)=T_{ZN}$$

$$T_{EE}=\frac{1}{\cos^2\varphi r^2}\left(\frac{\partial^2 T}{\partial\lambda^2}+r\cos^2\varphi\frac{\partial T}{\partial r}-\cos\varphi\sin\varphi\frac{\partial T}{\partial\varphi}\right)$$

$$T_{EZ}=\frac{1}{r\cos\varphi}\left(\frac{\partial^2 T}{\partial\lambda\partial r}-\frac{1}{r}\frac{\partial T}{\partial\lambda}\right)=T_{ZE}$$

$$T_{ZZ}=\frac{\partial^2 T}{\partial r^2}$$

where r is radial distance and φ, λ are latitude and longitude, respectively. All components except T_{ZZ} depend on the orientation of the planar coordinates (φ, λ), that is, the above field-operators (or field quantities) are not rotationally invariant. It is therefore useful to define rotationally invariant quantities such as the horizontal gradient and other invariant quantities such as the curvature and the total gradient (e.g. Pedersen & Rasmussen 1990). For the scope of illustration we take a spherical prism (spherical mass element bounded by two meridians, two latitudes and two spherical surfaces with radius r_1 and r_2) and map the gravity and T_{ZZ}. The prism has a side length of 100 km by 100 km, is 1 km thick, density 200 kg m^{-3} and its top is set at 4 km depth. The calculation height is 5000 m and is made in spherical coordinates. The two fields (Fig. 2) have the following characteristics: T_{ZZ} is centred on the mass, giving a positive signal over the body; along the borders of the body a small-amplitude negative stripe is observed. When the body is either deep or with slant borders, the negative stripe is reduced or absent. The gravity field is centred over the mass, but it does not show the negative values along the borders and the pattern of the anomaly is broader. We find that the T_{ZZ} component is ideal for geological mapping, as it highlights the centre of the anomalous mass with higher spatial resolution than gravity.

Main geological and tectonic features

The main geological features of interest in our study are shown in Figure 3. In north-central Africa, the West African Craton and the Sahara Metacraton have been identified (Abdelsalam *et al.* 2002). The southern part of the West African Craton consists of the Leo shield; its central part is the basement of the vast Taoudenni Basin. The Congo Craton dominates central Africa and its northern edge is seen in the south-eastern part of Figure 3. The African cratons are defined on the basis of their structural composition, age and

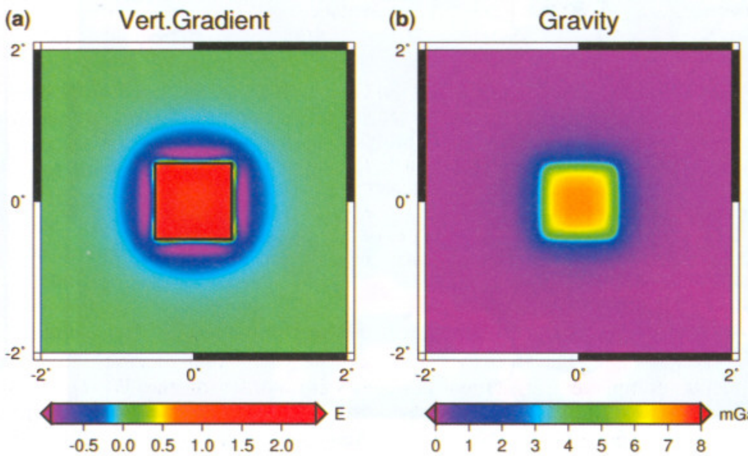

Fig. 2. (**a**) Vertical (T_{ZZ}) gradient and (**b**) gravity field over a spherical prism of size longitude = 1°, latitude = 1°, dz = 1 km, top at 4 km depth. Calculation height 5 km, density = 200 kg m^{-3}. The black box outlines the prism.

Fig. 3. Main geological features of north-central Africa. (**a**) Geologic map with the position of the profiles used in demonstrating fundamental differences in the gravity and gradient fields for the Chad lineament and the central African rift. Country names are shown. (**b**) Geographic index map with locations mentioned in the text and names of geological units shown in (a). The information stems from the Geologic map of Africa in six sheets (CGMW/UNESCO 1990). The outlines of cratons are based on numerous studies (e.g. Schlüter 2006; Priestley *et al.* 2008). The basin outlines coincide greatly with those of Persits *et al.* (2001). The principal rifts refer to Schlüter (2006), based on Guiraud *et al.* (2005). The magmatism relies on the works of Wilson & Guiraud (1992) and McHone (2000). CAR, central African rift; WAR, West African Rift; WCARS, west and central African rift system; Poli-rrr, position of the hypothetical Poli triple junction.

tectono-metamorphic evolution. They mostly comprise granite–gneiss complexes of greenstone belts associated with basic and ultra-basic rocks and of metamorphosed sediments.

On the eastern margin of the West African Craton, the Trans-Saharan Fold Belt of Pan-African age (Neoproterozoic) is located (Dauteuil *et al.* 2009). The Trans-Saharan Fold Belt marks the eastern border of the West African Craton and extends from Hoggar in the north to the Dahomeyides in the south. The fold belt is 100 to 400 km wide and 1300 km long, consisting of Pan-African meta-sediments. Along the fold belt a suture has been identified. It is marked by strings of mafic and ultra-mafic massifs in its southern and central portion. To the west of the Dahomeyides the overturned lower and middle sequences of the Volta Basin have been deformed and overthrusted, containing volcano–sedimentary complexes (Trompette 1994).

Volcanism in north-central Africa started in the Eocene (35–30 Ma) with the eruptions of the Hoggar magmatic province. The Cameroon line is a volcanic alignment oriented NNE–SSW that extends for more than 1000 km from Chad into the Atlantic Ocean. It was built between 32 Ma and the present day on a series of grabens and horsts which formed at the end of the Cretaceous (Dauteuil *et al.* 2009). The Tibesti volcanic province is emplaced on Precambrian basement; the volcanic activity seems to have started in the Lower Miocene and continued in the Quaternary (Gourgaud & Vincent 2004).

The west and central African rift system (WCARS) is a series of NNW–NW-trending extensional basins of the Early Cretaceous. The rift basins have widths greater than 150 km and depths in excess of 5 km. The WCARS lacks volcanism but is associated with a broad zone of crustal thinning (Fairhead & Green 1989). However, recent studies show that crustal thickness beneath the Cameroon volcanic line, beneath part of the WCARS and the Pan-African Oubanguides Belt, to the south is 35–39 km and the crust is even thicker under the northern margin of the Congo Craton (43–48 km) (Tokam *et al.* 2010). In our study area several large-scale intracratonic basins are found: the Chad, Taoudenni, Al Kufra and Murzuk basins. They are vast subsiding depressions, tectonically calm and developed on the Gondwana supercontinent (Dauteuil *et al.* 2009). Their relation to the crust and lithospheric structure has however not been studied in detail due to the absence of reliable data.

The modern gravity and gravity-gradient fields

Gravity and the components of the Marussi tensor are calculated for northern Africa starting from the EGM2008 (Pavlis *et al.* 2008) spherical harmonic expansion of the gravity potential field. We adopt a geocentric spherical coordinate system and calculate the fields at the height of 4000 m above a spherical Earth model of radius equal to the ellipsoidal radius at intermediate latitude (Earth radius 6375.37853 km; Janák & Šprlák 2006). The 4000 m height guarantees all values to be above topography, which is necessary for topographic reductions. The values are calculated on a regular grid of 0.05° (*c.* 6 km) grid cell size, with a maximum degree and order equal to 2159 of the harmonic expansion.

We correct the fields for the topographic effect. The topography is modelled with the ETOPO1 DEM (1 arc-minute global relief Digital Elevation model of Earth's surface; Amante & Eakins 2009) using a resolution of 0.02° (*c.* 2 km). We perform a spherical calculation, in which the spherical mass elements are approximated with a prismatic mass element (Forsberg 1984). We use a standard density of 2670 kg m^{-3} for land and a density of 1030 kg m^{-3} for the sea. The ETOPO1 grid is given in ellipsoidal geodetic coordinates, which must be converted into geocentric spherical coordinates for the calculations. The topography-corrected gravity anomaly and the vertical gradient (T_{ZZ}) are shown in Figure 4. The topographic correction removes the obvious correlation of the fields with the topography and produces the Bouguer anomaly field, if applied to the gravity anomaly. It is an analogous correction when applied to the vertical gradient. The correction amounts to up to a few hundreds of mGal for gravity and up to a few tens of Eötvös for the vertical gradient. It is greatest over the highest topographic elevations, for example the Tibesti massif.

Comparison of the gravity and the gradient field reveals that anomalies are located in the same regions, but that the gradient field highlights more details. Where the gravity shows either a negative or positive signal, the gradient is also anomalous but reflects shorter wavelengths and does not reproduce the same pattern. In the following we demonstrate the usefulness of the gradient field for highlighting geological features. The simplest way to achieve this task is to critically inspect the mapped fields, describe the characteristics and match them to the known geology. The correspondence between the characteristics of the field and the particular geological features allows us to apply the fields in other regions to reveal unknown structures that are either concealed by sediments or which have not been mapped before.

Large sag basins (e.g. Chad Basin) have low-gradient levels between -5 and $+5$ Eötvös for T_{ZZ} and are limited to -50 mGal for gravity. The volcanic deposits (e.g. Cameroon line, Tibesti massif) are distinct by high T_{ZZ} values exceeding $+30$ Eötvös. The gravity reflects the crustal thickness variations, and has either negative values as in Tibesti and Hoggar or positive values (schist belt of western Nigeria) lacking the short-wavelength characteristic of the gradient. Examples are the Tibesti massif, the Cameroon volcanic line and the Early Jurassic magmatic deposits of western Africa (compare Figs 3 & 4). Sutures generate a positive signal in T_{ZZ} (near to 30 Eötvös or slightly greater) and a positive gravity signal; the

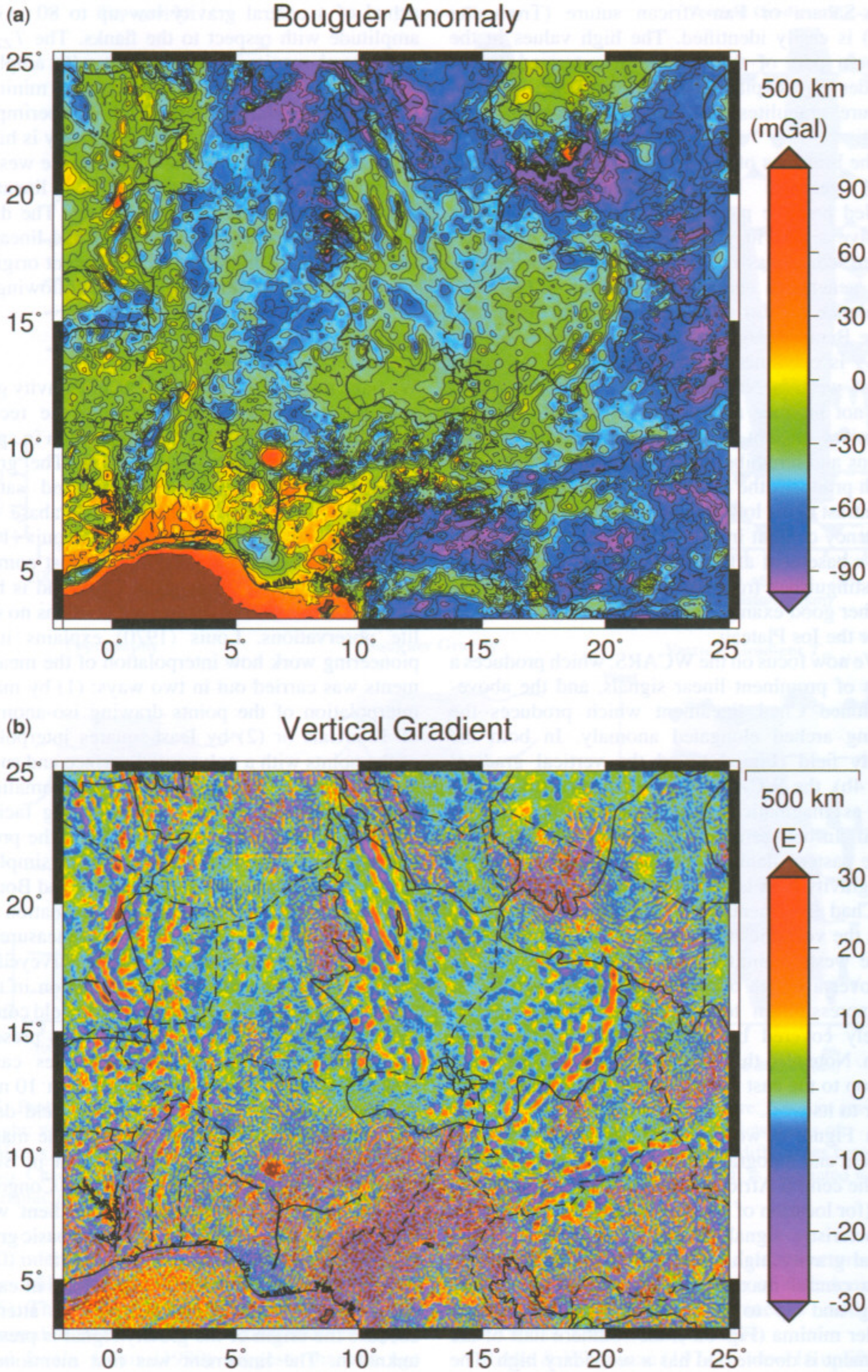

Fig. 4. (**a**) Bouguer gravity field in mGal and (**b**) vertical gradient corrected for topography in Eötvös units for the WCARS and the Chad lineament of north-central Africa. Outlines of major sedimentary basins depicted as continuous line; national borders depicted as dashed line.

Trans-Sahara or Pan-African suture (Trompette 1994) is easily identified. The high values in the southern part of the suture (also termed Dahomeyides) are explained by the presence of high-pressure granulites and eclogite (Attoh & Nude 2008).

The branches of the WCARS (Burke & Dewey 1972) generate linear gradient signals with coupled positive parallel anomalies in T_{ZZ} and a negative signal in gravity. Folded and metamorphosed sediments or basement with magmatic intrusions generate a characteristic signal in T_{ZZ}, with prevalence at short wavelengths. To the north-west of the Benue trough the short-wavelength content in T_{ZZ} is explained by the presence of the schist belt of western Nigeria (Trompette 1994), which does not produce a clear gravity signal. The belt comprises ancient basement intruded by granitic plutons and amphibolites, both high-density rocks, which produces the short-wavelength signal in T_{ZZ} in contrast to the lower density of schists. This high-frequency content in T_{ZZ} is very characteristic and allows basement affected by granitic intrusions to be distinguished from basement without intrusions. Another good example is given by the basement of Air or the Ios Plateau.

We now focus on the WCARS, which produces a series of prominent linear signals, and the above-mentioned Chad lineament which produces the striking arched elongated anomaly. In both the gravity field (Fig. 4a) and the vertical gradient (Fig. 4b), the WCARS can be clearly identified as well as magmatic deposits such as the Tibesti massif. In between the west and central rift zone, at the eastern flank of the Chad Basin, a slightly bent gravity high is observed which corresponds to the Chad lineament. This third linear signal connects the volcanic province of Tibesti in the north to the western limit of the CAR (central African rift) over a length of 1300 km. The lineament has no expression in topography or outcrop and is entirely covered by the sediments of the Chad Basin. Note also that it separates areas of basement outcrop to the east from areas of younger sediment cover to its west.

In Figure 5 we compare the gravity, gravity gradient and topography across the Chad lineament and the central African rift zone. The series of profiles (for location of profiles see Fig. 3a) reveals the characteristic signal of the Chad lineament: the central gravity high with over 50 mGal amplitude and a central maximum in T_{ZZ} up to 40 Eötvös strong and up to 75 km wide flanked by two smaller minima (Fig. 5a); the southern half of the lineament is double and has a secondary high. The topography is flat so the lineament is completely buried by sediments. The central African Rift (Fig. 5b) has a completely different characteristic signal of a central gravity low up to 80 mGal in amplitude with respect to the flanks. The T_{ZZ} has two lateral maxima 150 km apart with amplitude of up to 40 Eötvös strong and a central minimum. For the T_{ZZ} a relative central high is superimposed on the central minimum. The topography is high at one or the other sides of the rift. Both the west and central African rift systems are almost linear and are not bent like the Chad lineament. The differences in the characteristics of the Chad lineament and the WCARS highlight their different origin, as we will discuss in more detail in the following.

Discussion

We have mapped the gravity field and gravity gradients for central-north Africa using the recently available global potential field expansion in spherical harmonics (Pavlis *et al.* 2008). The gravity potential model blends terrestrial and satellite observations and has an increased database compared to the previous compilation of Louis (1970). To our knowledge, the latter is the most complete work on a gravity campaign in Chad and is based on a similar terrestrial dataset but contains no satellite observations. Louis (1970) explains in his pioneering work how interpolation of the measurements was carried out in two ways: (1) by manual interpolation of the points drawing iso-anomalies of 10 mGals or (2) by least-squares interpolation of the points with a polynomial surface and successive automatic drawing of the iso-anomalies at 10 mGal intervals. Available computing facilities three to four decades ago dictated that the processing and interpolation of the raw data be simplified.

The final maps of gravity anomaly and Bouguer anomaly therefore contain less information than the original observations that have a measurement error of 1–5 mGal, depending on the surveyed area (Louis 1970). The modern representation in terms of spherical harmonic expansion of the field contains locally more information than the maps presented by Louis (1970), as the iso-anomalies can be represented with a smaller interval than 10 mGal. A further improvement of the global field data is due to the geographical limitation of the maps of Louis (1970) that do not include data in Sudan, northern Chad, large parts of Nigeria or Congo.

We next consider the gravity gradient which highlights more superficial masses than basic gravity measurements.

The arcuate lineament 1300 km long in eastern Chad (Figs 3 & 4) deserves special attention, because the origin of the gravity signal is presently unknown. The lineament was first mentioned in Louis (1970), who describes the prominent gravity anomaly together with the other gravity highs and lows that can be found in Chad. Tentatively, Louis

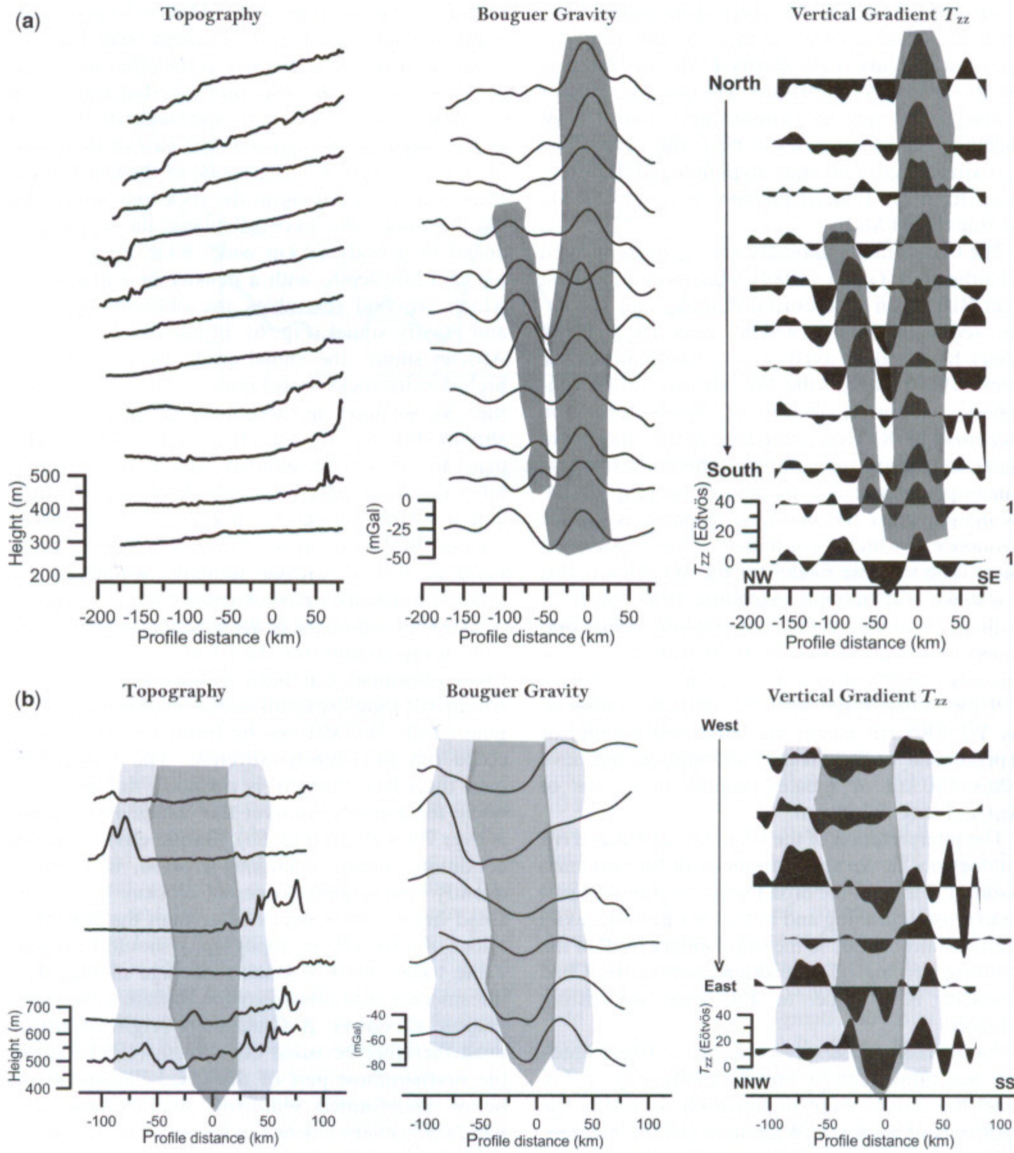

Fig. 5. Profiles comparing the central African rift with the Chad lineament. Left: topography; centre: Bouguer gravity; and right: vertical gravity gradient (dark shaded area depicts central axis; lighter shaded area depicts flanks of central axis). Profiles across (**a**) Chad lineament and (**b**) central African rift. Note the systematic differences between the two: Chad lineament has no topography and a gravity high associated with it, whereas the rift is associated with topographic highs along its flanks and is marked by a central gravity low.

(1970) interprets the anomaly as the western border of the Nile Craton, a block discussed by Rocci (1965). The lineament was interpreted to represent subcrustal material that was transferred to upper crustal levels. Louis (1970) suggests that the age of the feature is older than Cretaceous, and thus older than the Benue rift or the volcanism of Cameroon and Tibesti. The author considers it more probably related to a consolidated fracture with the presence of heavy elements of Caledonian or Precambrian age, contemporaneous with the Pan-African Trans-Saharan suture.

Burke & Whiteman (1973) review 16 uplifts and 25 rifts of Mesozoic and Tertiary age in Africa, including 11 rrr-junctions (rift–rift–rift junction produced by uplift). Among these the Poli rrr-junction (centred at 9°N, 14°E) is included, from which the Chad anomaly emanates, and which is suggested to mark a rift (termed Ati rift) forming one arm of the Poli structure. The positive gravity anomaly is interpreted (without any control from modelling) as a long series of basic intrusions. The approximate age of the three hypothesized rifts emanating from the Poli rrr-junction starts at 130 Ma and stops at 80 Ma.

The Chad gravity anomaly is roughly delineated in Fairhead & Green (1989) who model the East Niger Rift Basin with crustal thinning and successive sediment filling, which leads to a broad gravity high and an axial gravity low. Fairhead & Green (1989) explain the WCARS using the lithospheric extension model of basin formation (Mckenzie 1978). Here, stretching of the lithosphere results in passive upwelling of hotter less-dense asthenosphere and a concomitant necking of the low-density crust. The isostatic response is surface subsidence, which continues after extension ceases. The tectonic model for the WCARS is that of a strike–slip motion extending from the mid-ocean ridge along reactivated fracture zones into the Benue trough. The central African shear zone is ideally orientated to transmit strike–slip motion from the ocean ridge into the African continent. The WCARS rift basins are generated parallel or perpendicular to the shearing orientation and have widths 150 km or greater, depths in excess of 5 km and lack volcanism.

The interpretation of the Chad lineament as a rift arm does not fit the above framework for two main reasons: (1) it lacks the broad positive gravity signal due to crustal thinning and it does not have the axial gravity minimum due to the sedimentary infill of the subsiding rift; and (2) the orientation of the Chad lineament is oblique to the expected rifting direction.

An alternative interpretation of the Chad lineament was introduced by Freeth (1984) who tried to model the crustal dyke or intrusion following the hypothesis of Burke & Whiteman (1973). He concluded that an exceptionally and improbably great dimension of the dyke is needed to explain the gravity observations (over 1000 km length, 35 km width, *c.* 30 km thickness). The observed gravity signal also demonstrates abrupt changes, a feature easily explained by a superficial density contrast. Instead, the author proposed that the anomaly reflects the presence of a band of basic volcanic and/or volcanoclastic sediments within the basement, and therefore at shallower depths than the dyke or intrusions.

The gravity and gradient maps we present here highlight the fundamental differences between the Chad anomaly and the rifts in central-north Africa. The anomaly compares better to the Pan-African suture that borders the West African Craton, as it is particularly evident in the gradient field. The curvature radius of the lineament and the alignment next to reworked Precambrian basement are common features of the data. Two separate outcrops of the Saharan Metacraton to the east of the lineament fit the convex, eastern side of the Chad lineament and could belong to the rock unit limited by the lineament. We have calculated the signal produced by a body 30 km wide, 8 km thick and its top at 1 km depth, with a density of 300 kg m^{-3}, which we find resembles the observed gradient and gravity signal (Fig. 6). In analogy to the Pan-African suture, the signal could be generated by high-density rocks as eclogite, diorite or amphibolite. As we have no additional geophysical constraints, this is only one of many possible models that can explain the anomaly. However, the possibility that the anomaly is caused by crustal thinning and a superficial rift basin (the preferred model for the WCARS) can be ruled out (e.g. Browne & Fairhead 1983). Crustal thinning would clearly produce a gravity signal of greater wavelength.

Another argument is the absence of an expression in topography for the Chad lineament. If the Chad lineament had been formed by Cretaceous rifting, rift shoulder uplift would be observed analogous to the WCARS as the formation mechanism could not be entirely different. The topography over the Chad anomaly is perfectly flat (Fig. 5a), while the topography over the central African rift is over 700 m high (Fig. 5b). Similar environmental conditions imply analogous erosion, and consequently similar annual rates of erosion. Unless the Chad lineament is much older than the WCARS, traces of a rift-related topography should be observable today. Only a much older age of the Chad lineament would allow erosion to flatten the topographic elevation. A Cretaceous origin of rifting must therefore be ruled out. Freeth (1984) claims the northernmost part of the Chad lineament lies below undeformed sediments of Devonian age, which is further evidence in favour of the considerably older age than the Mesozoic rifts.

The interpretation of the Chad lineament in terms of an old structure due to the above argument is in good agreement with its geographical setting. The area we have investigated is part of the Saharan Metacraton defined by Abdelsalam *et al.* (2002): the crustal rocks occupying a rectangular-shaped region bounded by longitudes 8°30′E and 35°E and latitudes 3°N and 24°N. The metacraton relates to Neoproterozoic continental crust that has been remobilized during deformation, metamorphism, emplacement of igneous bodies and local episodes of crust formation related to rifting and oceanic basin development. The Saharan Metacraton is dominated by metamorphic rocks intruded

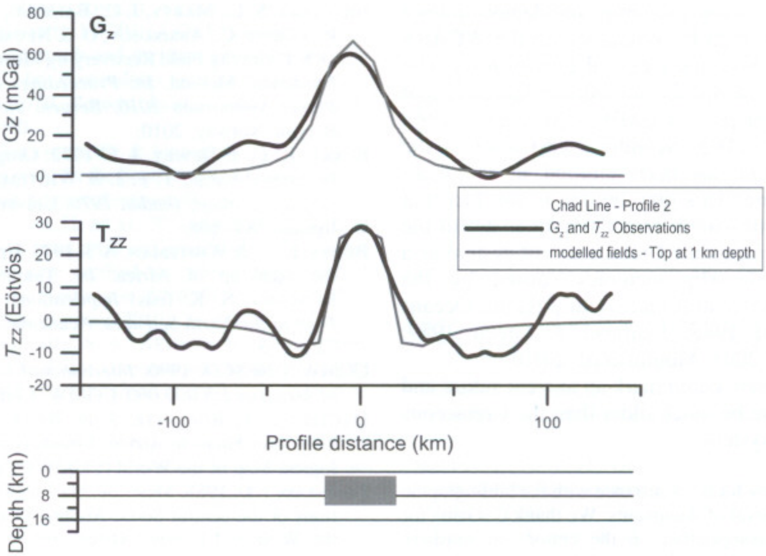

Fig. 6. Observed (black) and modelled (grey) vertical gradient (T_{ZZ}) and gravity field over a possible high density body (300 kg m^{-3} density, 30 km width, 8 km thickness, top at 1 km depth). The body represents one of many possible models. A deep origin of the observed signal in the Chad lineament can be excluded.

by Neoproterozoic granitoids ranging in age from 750 to 550 Ma. It seems that most of the gneisses were formed or metamorphosed during Neoproterozoic time, involving Palaeoproterozoic or even Archaean continental crust. Two structural trends dominate the Saharan Metacraton: an early ENE–WSW trend and a younger NS trend. The ENE–WSW trend would be compatible with the Chad lineament, and has been defined in the outcrops east of the Chad lineament as the Zalingei Fold Belt which is thought to continue SW into Cameroon. This trend has been interpreted as representing a pre-Neoproterozoic structure marked by an event of age 630–620 Ma, or was inherited from early Neoproterozoic terrane collisions. North-trending structures in the form of fold belts and faults have been found in some parts of the metacraton, as in the Tibesti massif. These north-trending upright folds and strike–slip faults were suggested to be due to east–west-aligned crustal shortening accompanying collision between the Saharan Metacraton and the Arabian–Nubian shield. In the context of crustal shortening, the Chad lineament could well be interpreted as overthrusted lower crust or high-grade compressional metamorphism that generated high-density rocks such as ultrabasics, eclogites and amphibolites.

Conclusions

The recent geodetic satellite missions CHAMP and GRACE have produced global observations of the gravity field with a resolution (half-wavelength) of 165 km. The integration with terrestrial data has resulted in a global gravity model with a nominal spatial resolution (half-wavelength) of about 10 km (Pavlis *et al.* 2008). The realistic resolution however depends on the availability of the terrestrial data and may change locally. We have mapped the vertical gravity gradient and the gravity field for north-central Africa and compared this field to existing geological maps and known tectonic structures. The gravity gradient is very well correlated to the geological map and to known lineaments such as fold belts, rifts and magmatic deposits associated with density variations. It shows that the global fields are suitable for tracing geological structures. The global availability makes direct access to any study area feasible. The advantage over regional or national databases is that possible datum shifts due to differences in reference systems are ruled out. Features extending several degrees can be traced, a task that may be difficult when combining several terrestrial databases. The use of the gradient fields is very valuable for highlighting superficial structures as deep structures are attenuated naturally by the potential field law of gravity (e.g. Blakely 1995).

A review of all major linear anomalies found in north-central Africa highlights a 1300 km long lineament which is comparable in amplitude to the well-known WCARS or the Trans-Sahara suture east of the Taoudenni Basin. It is a slightly arcuate linear feature, convex eastwards, running through Chad Basin to Tibesti. It has no topographic expression or geologic outcrop, and demonstrates a central gravity high in comparison to the WCARS rift (that demonstrates a central gravity low). The WCARS has entered the subsequent literature and geological maps (CGMW/UNESCO 1990; Guiraud *et al.* 2005; Schlüter 2006) whereas the Chad lineament has been omitted in the more recent literature. This may be due to the fact that its arcuate north–south orientation does not fit the model that explains the Cretaceous rift system as a result of strike–slip tectonics caused by the opening of the central and south Atlantic Oceans (e.g. Fairhead 1988; Fairhead & Green 1989; Guiraud *et al.* 2005; Moulin *et al.* 2010).

The lineament could mark an ancient suture and could therefore be much older than the Cretaceous WCARS rift system.

We thank I. Nagy for her assistance with the bibliographic search and retrieval of documents. We thank C. Gaina for providing the compilation on the cratons of northern Africa. We thank Statoil for financial support and in particular H. M. Bjørnseth from Statoil for discussions. We thank the Italian Space Agency (ASI) for supporting the GOCE-Italy project. The work was partially supported by PRIN contract 2008CR4455_003. We acknowledge the use of the GMT-mapping software of Wessel & Smith (1998) and the tesseroid forward calculation software developed by L. Uieda in the frame of our GOCE-projects. We acknowledge the use of the EGM2008 gravity model and software of Pavlis *et al.* (2008). We thank R. Rummel, C. Reeves and the editor S. Buiter for their meticulous reviews.

References

ABDELSALAM, M. G., LIEGEOIS, J.-P. & STERN, R. J. 2002. The Saharan metacraton. *Journal of African Earth Sciences*, **34**, 119–136.

AMANTE, C. & EAKINS, B. W. 2009. ETOPO1 1 Arc-Minute Global Relief Model: Procedures, Data Sources and Analysis. NOAA Technical Memorandum NESDIS NGDC-24, 19, March 2009.

ATTOH, K. & NUDE, P. M. 2008. The tectonic significance of carbonatite and ultra-high pressure rocks in the Pan-African Dahomeyide suture zone, southeastern Ghana. *In*: ENNIH, N. & LIEGEOIS, J.-P. (eds) *The Boundaries of the West African Craton*. Geological Society, London, Special Publications, **297**, 217–231.

BLAKELY, R. J. 1995. *Potential Theory in Gravity and Magnetic Applications*. Cambridge University Press, Cambridge.

BRAITENBERG, C. & EBBING, J. 2009. New insights into the basement structure of the west-Siberian basin from forward and inverse modelling of Grace satellite gravity data. *Journal of Geophysical Research*, **114**, B06402, doi: 10.1029/2008JB005799.

BROWNE, S. E. & FAIRHEAD, J. D. 1983. Gravity study of the Central African Rift System: a model of continental disruption. The Ngaoundere and Abu Gabra rifts. *Tectonophysics*, **94**, 187–203.

BRUINSMA, S. L., MARTY, J. C., BALMINO, G., BIANCALE, R., FÖRSTE, C., ABRIKOSOV, O. & NEUMAYER, H. 2010. GOCE Gravity Field Recovery by Means of the Direct Numerical Method. *In*: *Proceedings of ESA Living Planet Symposium 2010, Bergen, June 27–July 2*, Bergen, Norway, 2010.

BURKE, K. C. & DEWEY, J. F. 1972. Orogeny in Africa. *In*: DESSAUVAGIE, T. F. J. & WHITEMAN, A. J. (eds) *African Geology, Ibadan 1970*. University of Ibadan, Ibadan, 583–608.

BURKE, K. C. & WHITEMAN, A. J. 1973. Uplift, rifting and the break-up of Africa. *In*: TARLING, D. H. & RUNCORN, S. K. (eds) *Implications of Continental Drift to the Earth Sciences*. Academic Press, London, 735–755.

CGMW/UNESCO. 1990. *International Geological Map of Africa at 1:5 000 000*. CGMW/UNESCO, Paris.

DAUTEUIL, O., BOUFETTE, J. & TOTEU, F. 2009. *The Changing Faces of Africa*. Commission for the Geological Map of the World (CGMW), Paris, 1–48.

FAIRHEAD, J. D. 1988. Mesozoic plate tectonic reconstructions of the central South Atlantic Ocean: the role of the West and Central African rift system. *Tectonophysics*, **155**, 181–191.

FAIRHEAD, J. D. & GREEN, C. M. 1989. Controls on rifting in Africa and the regional tectonic model for the Nigeria and east Niger rift basins. *Journal of African Earth Sciences*, **8**, 231–249.

FORSBERG, R. 1984. *A study of terrain reductions, density anomalies and geophysical inversion methods in gravity field modelling*. Ohio State University, Scientific Report No. 5, Report Number AFGL-TR-84-0174, 133.

FÖRSTE, C., SCHMIDT, R. *ET AL.* 2008. The GeoForschungsZentrum Potsdam/Groupe de Recherche de Gèodésie Spatiale satellite-only and combined gravity field models: EIGEN-GL04S1 and EIGEN-GL04C. *Journal of Geodesy*, **82**, 331–346, doi: 10.1007/s00190-007-0183-8.

FREETH, S. J. 1984. How many rifts are there in West Africa? *Earth and Planetary Science Letters*, **67**, 219–227.

GOURGAUD, A. & VINCENT, P. M. 2004. Petrology of two continental alkaline intraplate series at Emi Koussi volcano, Tibesti, Chad. *Journal of Volcanology and Geothermal Research*, **129**, 261–290.

GUIRAUD, R., BOSWORTH, W., THIERRY, J. & DELPLANQUE, A. 2005. Phanerozoic geological evolution of Northern and Central Africa: an overview. *Journal of African Earth Sciences*, **43**, 83–143.

HOFMANN-WELLENHOF, B. & MORITZ, H. 2005. *Physical Geodesy*. Springer, Berlin.

JANÁK, J. & ŠPRLÁK, M. 2006. New software for gravity field modelling using spherical harmonics. *Geodetic and Cartographic Horizon*, **52**, 1–8 (in Slovak).

LOUIS, P. 1970. Contribution geophysique à la connaissance géologique du basin du lac Tschad. *Memoires Orstom*, **42**, 1–311.

MCHONE, J. G. 2000. Non-plume magmatism and rifting during the opening of the central Atlantic Ocean. *Tectonophysics*, **316**, 287–296.

MCKENZIE, D. 1978. Some remarks on the development of sedimentary basins. *Earth and Planetary Science Letters*, **40**, 25–32.

MIGLIACCIO, F., REGUZZONI, M., SANSÒ, F., TSCHERNING, C. C. & VEICHERTS, M. 2010. GOCE data analysis: the space-wise approach and the first space-wise gravity field model. *In*: *Proceedings of ESA Living Planet Symposium 2010, Bergen, June 27–July 2*, Bergen, Norway, 2010.

MOULIN, M., ASLANIAN, D. & UNTERNEHR, P. 2010. A new starting point for the South and Equatorial Atlantic Ocean. *Earth-Science Reviews*, **98**, 1–37.

PAIL, R., GOIGINGER, H. ET AL. 2010. GOCE gravity field model derived from orbit and gradiometry data applying the time-wise method. *In*: *Proceedings of ESA Living Planet Symposium 2010, Bergen, June 27–July 2*, Bergen, Norway, 2010.

PAVLIS, N. K., HOLMES, S. A., KENYON, S. C. & FACTOR, J. K. 2008. An Earth Gravitational Model to degree 2160: EGM2008. *Geophysical Research Abstracts*, **10**, EGU2008-A-01891.

PEDERSEN, L. B. & RASMUSSEN, T. M. 1990. The gradient tensor of potential field anomalies: some implications on data collection and data processing of maps. *Geophysics*, 1558–1566.

PERSITS, F. M., AHLBRANDT, T. S., TUTTLE, M. L., CHARPENTIER, R. R., BROWNFIELD, M. E. & TAKAHASHI, K. I. 2001. *Maps showing geology, oil and gas fields and geological provinces of Africa*, Open file report 97–470A, Version 2.0, US Department of Interior, US Geological Survey.

PRIESTLEY, K., MCKENZIE, D., DEBAYLE, E. & PILIDOU, S. 2008. The African upper mantle and its relationship to tectonics and surface geology. *Geophysical Journal International*, **175**, 1108–1126.

ROCCI, G. 1965. Essai d'interprétation de measures géochronologiques: la structure de l'Ouest africain. *Sciences de la Terre*, **10**, 462–478.

RUMMEL, R., BALMINO, G., JOHANNESSEN, J., VISSER, P. & WOODWORTH, P. 2002. Dedicated gravity field missions-principles and aims. *Journal of Geodynamics*, **22**, 3–20.

SCHLÜTER, T. 2006. *Geological Atlas of Africa*. Springer Verlag, Berlin.

TOKAM, A. P. K., TABOD, C. T., NYBLADE, A. A., JULIÀ, J., WIENS, D. A. & PASYANOS, M. E. 2010. Structure of the crust beneath Cameroon, West Africa, from the joint inversion of Rayleigh wave group velocities and receiver functions. *Geophyical Journal International*, **183**, 1061–1076.

TROMPETTE, R. 1994. *Geology of Western Gondwana (2000–500 Ma)*. Balkema A. A. Publishers, Rotterdam, 1–350.

WESSEL, P. & SMITH, W. H. F. 1998. New, improved version of generic mapping tools released. *Transactions of American Geophysical Union*, **79**, 579.

WILSON, M. & GUIRAUD, R. 1992. Magmatism and rifting in Western and Central Africa, from Late Jurassic to Recent times. *Tectonophysics*, **213**, 203–225.